J Physiol (2003), **546.2**, *pp.* 551–564
DOI: 10.1113/jphysiol.2002.029751

www.jphysiol.org

Journal of Physiology

Uptake of locally applied deoxyglucose, glucose and lactate by axons and Schwann cells of rat vagus nerve

Céline Véga*, Jean-Louis Martiel†, Delphine Drouhault, Marie-France Burckhart‡ and Jonathan A. Coles

*Unité mixte INSERM/UJF/LRC-CEA U438, Centre Hospitalier Universitaire de Grenoble, 38043 Grenoble, *INSERM U394, Institut François Magendie, Bordeaux and †TIMC-TIMB, UMR CNRS 5525, Grenoble and ‡Service d'Imagerie, CRSSA, Grenoble, France*

We asked whether, in a steady state, neurons and glial cells both take up glucose sufficient for their energy requirements, or whether glial cells take up a disproportionate amount and transfer metabolic substrate to neurons. A desheathed rat vagus nerve was held crossways in a laminar flow perfusion chamber and stimulated at 2 Hz. ^{14}C-labelled substrate was applied from a micropipette for 5 min over a < 0.6 mm band of the surface of the nerve. After 10–55 min incubation, the nerve was lyophilized and the longitudinal distribution of radioactivity measured. When the weakly metabolizable analogue of glucose, 2-deoxy-[U-^{14}C]D-glucose (*DG), was applied, the profiles of the radioactivity broadened with time, reaching distances several times the mean length of the Schwann cells (0.32 mm; most of the Schwann cells are non-myelinating). The profiles were well fitted by curves calculated for diffusion in a single compartment, the mean diffusion coefficient being 463 ± 34 μm^2 s^{-1} (± S.E.M., n = 16). Applications of *DG were repeated in the presence of the gap junction blocker, carbenoxolone (100 μM). The profiles were now narrower and better fitted with two compartments. One compartment had a coefficient not significantly different from that in the absence of the gap junction blocker (axons), the other compartment had a coefficient of 204 ± 24 μm^2 s^{-1}, n = 4. Addition of the gap junction blocker 18-α-glycyrrhetinic acid, or blocking electrical activity with TTX, also reduced longitudinal diffusion. Ascribing the compartment in which diffusion was reduced by these treatments to non-myelinating Schwann cells, we conclude that 78.0 ± 3.6 % (n = 9) of the uptake of *DG was into Schwann cells. This suggests that there was transfer of metabolic substrate from Schwann cells to axons. Local application of [^{14}C]glucose or [^{14}C]lactate led to variable labelling along the length of the nerve, but with both substrates narrow peaks were often present at the application site; these were greatly reduced by subsequent treatment with amylase, a glycogen-degrading enzyme.

(Resubmitted 30 July 2002; accepted after revision 24 October 2002; first published online 22 November 2002)
Corresponding author J. A. Coles: INSERM U438, CHU, Pavillon B, BP 217, 38043 Grenoble cedex 9, France.
Email: jonathan.coles@ ujf-grenoble.fr

Lactate is a major intermediate of glucose metabolism in normoxic neural tissue as it is in normoxic muscle (see, e.g. Brooks, 2002). In early work on brain slices (e.g. McIlwain, 1953) it seemed possible that lactate was produced in an anoxic core, but this was unlikely for a preparation as small as a sympathetic ganglion (Larrabee, 1992), and tests made by Véga *et al.* (1998) showed that it was not the case for vagus nerve. Most strikingly, when [^{13}C]glucose is infused in anaesthetized rats, lactate is the first compound in the brain whose labelling is detected by NMR (Pfeuffer *et al.* 1999). Lactate is released from neural tissue (e.g. Larrabeee, 1992; Véga *et al.* 1998), and, as sole metabolic substrate, supports energy metabolism in sympathetic ganglia (Larrabee & Horowicz, 1956) and electrical activity in hippocampal slices (Schurr *et al.* 1988) and optic nerve (Wender *et al.* 2000). It is therefore clear that lactate is transferred between cells in nervous tissue: the question we address here is whether this transfer is directed from one cell type to another, and, if so, the quantitative contribution of this transfer to the metabolism of neurons. Present evidence includes the observation that during glucose deprivation there appears to be a net transfer of lactate from glial cells to neurons of rat optic nerve as glial glycogen is degraded (Wender *et al.* 2000). Experiments, mainly on isolated or cultured cells, have led to the suggestion that even in the presence of glucose, lactate is released by glial cells and taken up by neurons (Walz & Mukerji, 1988; Dringen *et al.* 1993*a*; Pellerin & Magistretti, 1994; Tsacopoulos & Magistretti, 1996), the most direct evidence being for the special case of the inner segments of mammalian photoreceptors (Poitry-Yamate *et al.* 1995). An *in vivo* result that supports the hypothesis is that lactate injected in the blood stream of rats is metabolized in the brain mainly by neurons, not astrocytes (Bouzier *et al.* 2000). Arguments against uncritical acceptance of the hypothesis have been presented by Chih *et al.* (2001) and by Gjedde *et al.* (2002).

If the hypothesis that neurons receive much of their carbon fuel from glial cells is correct, then glial cells must take up more glucose than is necessary for their own energy requirements, which are thought to be much less than those of neurons (Attwell & Laughlin, 2001). A useful tool for studying the uptake of glucose is its analogue, 2-deoxy-D-glucose (DG), which is transported on glucose transporters, and converted within cells to DG-6P. DG-6P is only metabolized slowly, mainly to DG-1-6P_2 and DG-1P; there is also weak incorporation into glycogen (Nelson *et al.* 1984; Dienel & Cruz, 1993). These products of DG are trapped within the cells that took up DG, so, if radioactively labelled DG (*DG) is supplied to a tissue, regions of increased metabolic activity can be mapped by autoradiography (^{3}H, ^{14}C, Sokoloff *et al.* 1977) or by positron emission tomography (^{18}F, Fox *et al.* 1988). A limitation to a detailed understanding of the results is that identification, in mammalian nervous tissue other than the retina, of the type of cell that takes up the DG, has proved difficult, although recently a promising new method has been developed (Wittendorp-Rechenmann *et al.* 2002).

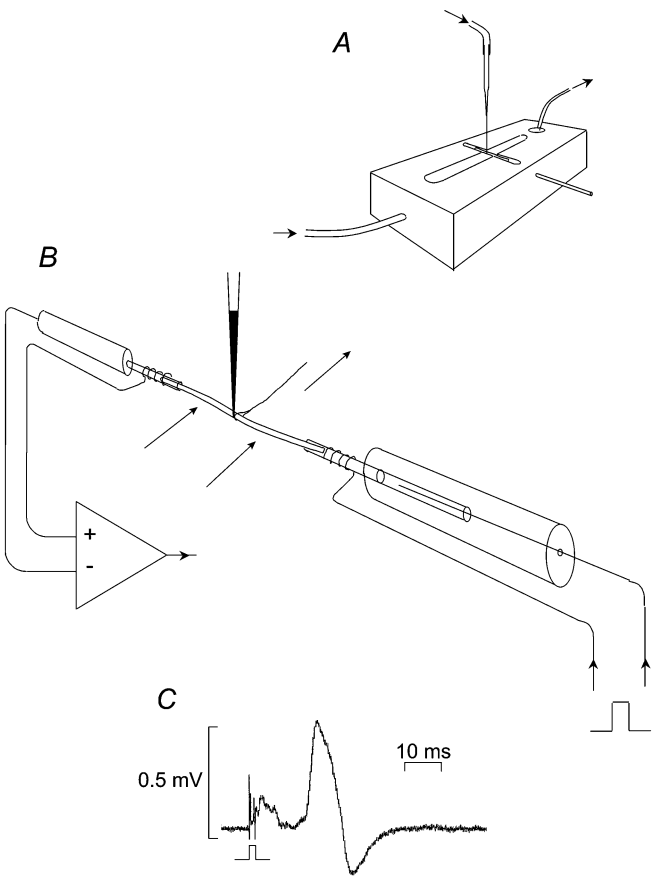

Figure 1. Local application of radioactive compounds

A, the perfusion chamber with lateral arms in which a length of nerve was mounted crossways. *B*, scheme of application from a micropipette of solution containing ^{14}C-labelled substrate. The ends of the nerve are sucked into capillaries equipped with wires for stimulating and recording. *C*, example of a compound action potential, recorded 41 min after the nerve was mounted. The small component from myelinated fibres appears with a peak at about 3 ms; it is followed by the larger, partly biphasic, component from unmyelinated fibres.

In order to identify the types of cell that take up 2DG in a mammalian nervous tissue, and to estimate the relative amounts taken up by the different types of cell, we have used a peripheral nerve. This conveniently contains long neuronal processes (axons) and relatively short ensheathing glial cells (Schwann cells) and we expected that we could determine whether ^{14}C-labelled compounds were within the axons or within the Schwann cells by applying *DG at one point and measuring the diffusion of radioactive products along the nerve. The cervical vagus nerve (of the rat) was chosen because more than 80 % of the axons, although ensheathed by Schwann cells, are small and not myelinated (Soltanpour & Santer, 1996) and therefore have a high metabolic rate per unit weight (Ritchie & Straub, 1956). It has been shown that the desheathed vagus nerve of rabbit releases lactate from regions that are not hypoxic, and can take it up and metabolize it (Véga *et al.* 1998), and lactate release from rat sciatic nerve has also been observed (C. Véga and S. Langle, unpublished results). We also describe experiments in which [^{14}C]glucose or [^{14}C]lactate were applied in the same way.

METHODS

Perifusion of the vagus nerve

The cervical vagus nerves of male Wistar rats, 220–270 g, 7–9 weeks old were used. The dissection was carried out in conformity with the guidelines of French Government decree 87-848, 19 October 1987, under experimenter licences 006683 and A38071. The rat was placed in a plastic box supplied with air containing 4 % halothane from a mixing device (Fluotec 3, Cyprane Ltd, Keighley, UK). When the rat was immobile, it was given an intraperitoneal injection of chloral hydrate (400 mg (kg body wt)$^{-1}$). After the nerves had been dissected out the rat was killed by injection of air in a femoral vein. The nerves were placed in Locke solution containing (mM): NaCl, 154; KCl, 5.6; $CaCl_2$, 0.9; $MgCl_2$, 0.5; glucose, 5; Hepes buffer, 10; pH adjusted to 7.4. The solution was air-equilibrated, pre-cooled to 4 °C and maintained at this temperature during storage for up to 6 h. Just before use, the connective tissue surrounding a length of nerve (8–15 mm long) was pulled off in one piece. A rabbit vagus nerve desheathed in this way and examined by electron microscopy was found to lack its perineurium; the endoneurium, consisting of axons ensheathed by Schwann cells that were well separated by collagen-filled space, was either directly in contact with the bath, or separated from it in places by a loose epineurium.

A perfusion chamber (Fig. 1*A*) was made from Perspex, with two lateral arms in which were suction electrodes (glass capillary tubes with one end narrowed by melting to an internal diameter of 0.20–0.28 mm). The suction electrodes held the nerve so that it was perpendicular to the flow. The design of the chamber was adjusted so that the flow of the perfusate round the central part of the nerve had no lateral component: the chamber was deep (7 mm), its floor had rounded sides and the flow rate was only about 2 ml min^{-1}. The stimulating pulse was adjusted (duration, 1–10 ms; amplitude, 1.5–8 V) to give a compound action

potential with maximum amplitude of the large C component. This action potential was recorded on a chart recorder with a memory (WR7600, Graphtek, Tokyo; Fig. 1*C*). Except when noted, the nerve was stimulated at 2 Hz throughout the experiment, the aim being to impose a high, defined, level of activity, and to avoid an uncontrollable amount of activity induced by the depolarization at the cut ends of the nerve. Nerves showing low conduction velocities, such that the time from the stimulus to the zero-crossing of the unmyelinated-fibre component was greater than 30 ms, were excluded. Parallel experiments had shown that the action potential was maintained for up to at least 30 min in glucose-free Locke solution equilibrated with air, and that increasing the O_2 content of the Locke solution, or adding 1% Evans blue, did not noticeably change the electrical activity.

Local application of labelled substrates

The labelled substrates, with the activity given by the manufacturer, were: 2-deoxy-[U-^{14}C]D-glucose, 11.5 GBq mmol^{-1} (*DG, NEN Life Science Products); [1-^{14}C]D-glucose, 2.1 GBq mmol^{-1} (*glucose) and Na[U-^{14}C]L-lactate, 5.6 GBq mmol^{-1} (*lactate) (Amersham Pharmacia Biotech). Solutions were prepared of glucose-free Locke solution containing 1 mg (100 μl)$^{-1}$ Evans blue and 1–5 mM labelled substrate. A glass micropipette was pulled from capillary tubing with a filament and the tip broken to 15–20 μm internal diameter. The tip was back-filled with the labelled solution and a tube fitted to the back so that pressures up to 5 bar could be applied (by a head of water, a syringe or from a gas cylinder). The nerve was placed in the chamber, which was perfused with glucose-free Locke solution. The micropipette was fixed on a micromanipulator and the tip inserted in the bath. The back pressure was adjusted to eject a fine plume, made visible by the Evans blue. (To avoid contaminating the nerve, this was done downstream of the nerve.) After the nerve had been washed for 5 min by the glucose-free solution, the pipette was moved close to the upstream side of the nerve so that the plume flowed over the surface of the nerve, usually both the upper and lower surfaces but, in earlier experiments, only one surface (Fig. 1*B*). Application was stopped by removing the pipette, usually after 5 min. The perfusate was switched to Locke solution containing 5 mM glucose for an incubation period, usually of 10, 25 or 55 min, to allow radioactive compounds to diffuse along the nerve. The nerve was then ejected gently from the suction electrodes and, to minimize stretching, drawn out through the meniscus of the bath on a piece of aluminium foil. The nerve, supported by the foil, was frozen in liquid nitrogen and lyophilized for 3–15 h.

Profiles of radioactivity

Lyophilized nerves were aligned on a microscope slide and the distribution of the radioactivity recorded by covering the nerves with a sheet of scintillant, which was observed by an intensifying digital camera (Micro Imager, Biospace Mesures, Paris). The acquisition of the image could be observed in real time; counts collected over 1–5 days were usually considered sufficient to reduce shot noise below other sources of error. Using the program Betavision 4.2 (Biospace), a strip of image including the nerve was selected and the profile of the counts along this strip obtained with a pixel size of 10 μm × 10 μm. The mean background noise was measured in an area of the field away from nerves and subtracted from the profiles. For some of the figures (e.g. Fig. 5*B*), profiles were smoothed by digital low-pass filtering. Six nerves that had been exposed to *DG, and whose profiles had been recorded, were partially digested with trypsin and placed in a conventional scintillation counter which recorded 554 ± 241 counts min^{-1} nerve^{-1} (mean ± S.E.M.).

To test for the presence of glycogen or protein in radioactive peaks, lyophilized nerves were incubated for 1–3 h at 37 °C with either α-amylase (1,4-α-D-glucan glucanohydrolase; E.C. 3.2.1.1, Sigma A-6380, 1–2 mg ml^{-1} Locke solution, pH 6.9) or trypsin (Sigma T-4665, 1.5 mg ml^{-1}): the nerves were then washed at room temperature for 5 min, lyophilized and placed again in the Micro Imager. As controls, nerves were treated in the same way with Locke solution.

Length of non-myelinating Schwann cells

A nerve was treated for 30 min with trypsin (3 mg ml^{-1}), then fixed with 4% paraformaldehyde, and the fibres spread apart. Nuclei were stained with Hoechst 33342, and the number of nuclei per millimetre length was counted. This number was divided into the number of Schwann cells in a cross section of the nerve, as estimated from electron micrographs. This procedure gave a mean length of 0.32 mm, somewhat longer than earlier measurements on teased nerve fibres (Peyronnard *et al.* 1975).

Drugs

Halothane was added by weight to Locke solution and shaken vigorously. Carbenoxolone (Sigma) was added as a stock solution. 18-α-glycyrrhetinic acid (αGA, Sigma) was dissolved in dimethylsulphoxide (DMSO) at 100 mM, and added drop by drop to Locke solution at about 40 °C that was stirred for about 1 h until the αGA redissolved. Control experiments were carried out with DMSO alone (10^{-4} v/v). TTX (Tocris) was stored at −20 °C as a stock solution. α-cyano-4-hydroxy-cinnamic acid (Sigma C-2020) was dissolved, with prolonged stirring, in the Locke solution and the pH re-adjusted.

Analysis of radioactivity profiles

Nerve profiles (such as Fig. 2*C*) were handled in Excel 5.0 (Microsoft) and Kaleidagraph 3.08 (Synergy Software). The equations used to describe the diffusion of labelled compounds along the nerve are given in the Appendix. Nerve profile 193 (nominally for an application of *DG in the presence of TTX) had a width that differed from the mean of the others of this class by 7.7 times the S.D. and was excluded. In addition, the procedure for fitting profiles did not converge in some cases (e.g. when the profile was asymmetric). Errors are expressed as S.E.M. and populations were compared using Student's two-tailed *t* test.

RESULTS

Distribution of radioactivity after localized uptake of *DG

A desheathed vagus nerve was suspended crossways in the laminar-flow chamber (Fig. 1*A*). It was stimulated continuously at 2 Hz, a frequency that is estimated to increase energy requirements by a factor of about 11 above the resting requirements (Ritchie, 1967; Fig. 1*C*). The perfusate was switched from normal Locke solution to glucose-free solution for 5 min, then a narrow band of the surface of the nerve was exposed to a solution of glucose-free Locke solution to which had been added 1 mM *DG and Evans blue (to make it visible; Fig. 1*B*). The application lasted 5 min, and then the nerve was perifused with Locke solution containing 5 mM unlabelled glucose for 25 min, frozen and lyophilized. The width of the mark left by the Evans blue (190–600 μm) was measured (Fig. 2*A*): it appeared to correspond well (to within about

100 μm) to the width directly exposed to the application, and did not become wider during the incubation. The profile of the distribution of radioactivity along the lyophilized nerve (Fig. 2*B*) had a bell-shaped peak centred on the point of application (Fig. 2*C*). Because we were incapable of reliably controlling the effectiveness of the application, we paid little attention to the absolute amount of radioactivity in the nerve; we did, however, observe that if the application was made while the nerve was perifused with solution containing 5 mM glucose, very much less radioactive substrate was taken up ($n = 2$). As expected, the detected β emission was mainly from the superficial layers of the lyophilized nerve: when a second, unlabelled, lyophilized, nerve was placed over the radioactive peak of a lyophilized nerve, the peak was still detected but with its amplitude decreased below 10 %, i.e. most of the radiation from the underside of a nerve was absorbed before reaching the scintillant film.

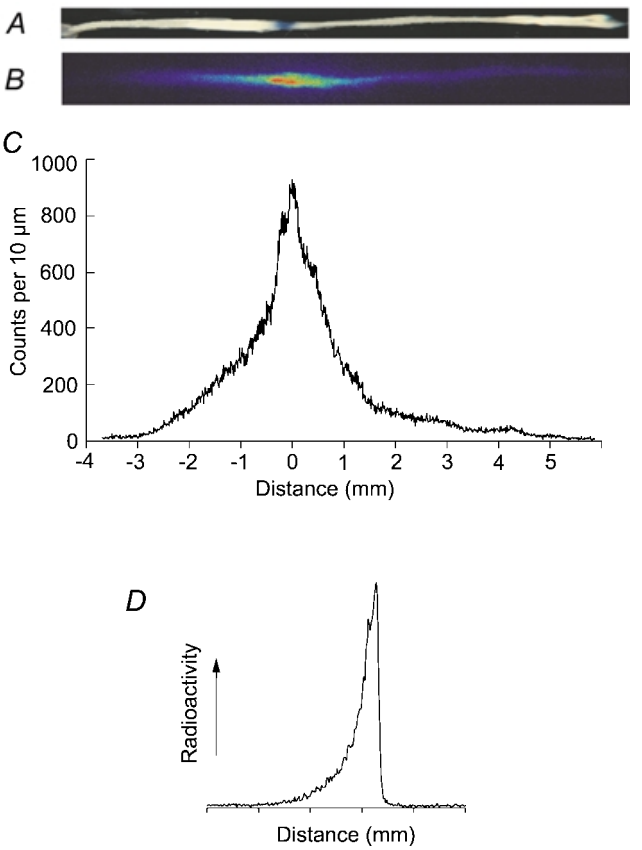

Figure 2. Imaging the distribution of radioactivity

Solution containing 2-deoxy-[U-^{14}C]D-glucose (*DG) and Evans blue was applied to a narrow band of nerve for 5 min and the nerve was then incubated for 55 min and lyophilized; the mark left by the Evans blue is visible on the lyophilized nerve (*A*). The radioactivity was imaged for 121.5 h (*B*). A profile was obtained for a strip 580 μm wide with a longitudinal resolution of approximately 10 μm (*C*). To check the spatial resolution of the method, *DG was applied to the cut end of a nerve (*D*). In this case, *DG was applied for 10 min and the nerve was washed for 19 min before being frozen.

The profile of radioactivity in Fig. 2*C* (presumably mainly *DG-6P) extended over several times the width of the Evans blue mark and several times the mean length of the Schwann cells (0.32 mm, see Methods), but much less than the length of the axon. To check that this spread was not an artefact due to poor spatial resolution of the radio imaging, we created an abrupt step of radioactivity by applying *DG to the cut end of a nerve. Figure 2*D* shows that this step was faithfully imaged with 10–90 % rise in less than 83 μm, a distance small compared to the width of the other profiles.

When the incubation time after local application of *DG was varied, the profiles of the radioactivity were found to become wider with time (Fig. 3*A*). As a preliminary characterization of the spread we measured the width at 30 % of the peak height (*W*30). *W*30 is plotted against time up to 60 min from the beginning of the *DG application in Fig. 3*B* (squares). The mean width of the Evans blue mark is indicated by the height of the rectangular box, and the duration of the *DG application by its length. Other features of Fig. 3*B* will be considered later.

Effect of gap junction blockers on the profiles of radioactivity

Schwann cells of mouse vagus nerve express gap junction proteins (Connexin 32 and Connexin 43; Zhao *et al.* 1999) and there is electrical and dye coupling between the glial cells (astrocytes) that ensheathe the axons of amphibian optic nerve (Cohen, 1970; Marrero & Orkand, 1996). When the blocker of gap junctions, (αGA, 10 μM; Davidson & Baumgarten, 1988), was included in the perifusate, the profiles of radioactivity were narrower than those in the carrier, DMSO (Fig. 3*C*). To compare profiles using all the information available (the whole profile, the width of the Evans blue mark, and the finite length of the nerve) we used the program described in the Appendix to fit each profile with a curve describing diffusion in a single compartment with a diffusion coefficient *D* (see Fig. 4*A*). There were significant reductions in *D* with αGA ($P = 0.011$, compared to the carrier, DMSO), and also with the related more water-soluble gap junction blocker, carbenoxolone (100 μM, $P = 0.0069$). Halothane (3 mM, Rozental *et al.* 2001) did not significantly reduce *D* compared to control nerves, but did reduce it compared to nerves exposed to DMSO, another organic solvent. These results are summarized in Fig. 3*D*. The carbenoxolone was added only during the incubation period; the αGA and the halothane were present also during the application of *DG.

Effect of TTX

We had chosen for the control conditions electrical stimulation at 2 Hz in the absence of drugs. We found that when 1 μM TTX was included in the perfusion solutions, so that both stimulated action potentials, and any possible spontaneous ones, were eliminated, the spread of *DG and

its products was reduced, much as in the presence of carbenoxolone (Fig. 3*D*, $P = 0.021$ for the decrease in *D* at 30 min after the beginning of the *DG application). TTX also reduced *W*30 and *D* at 15 and 60 min (triangles in Fig. 3*B*).

Analysis of the radioactivity profiles after application of *DG

The profiles obtained in control conditions (electrical stimulation at 2 Hz) were in general well-fitted by the theoretical curve for one dimensional diffusion of molecules,

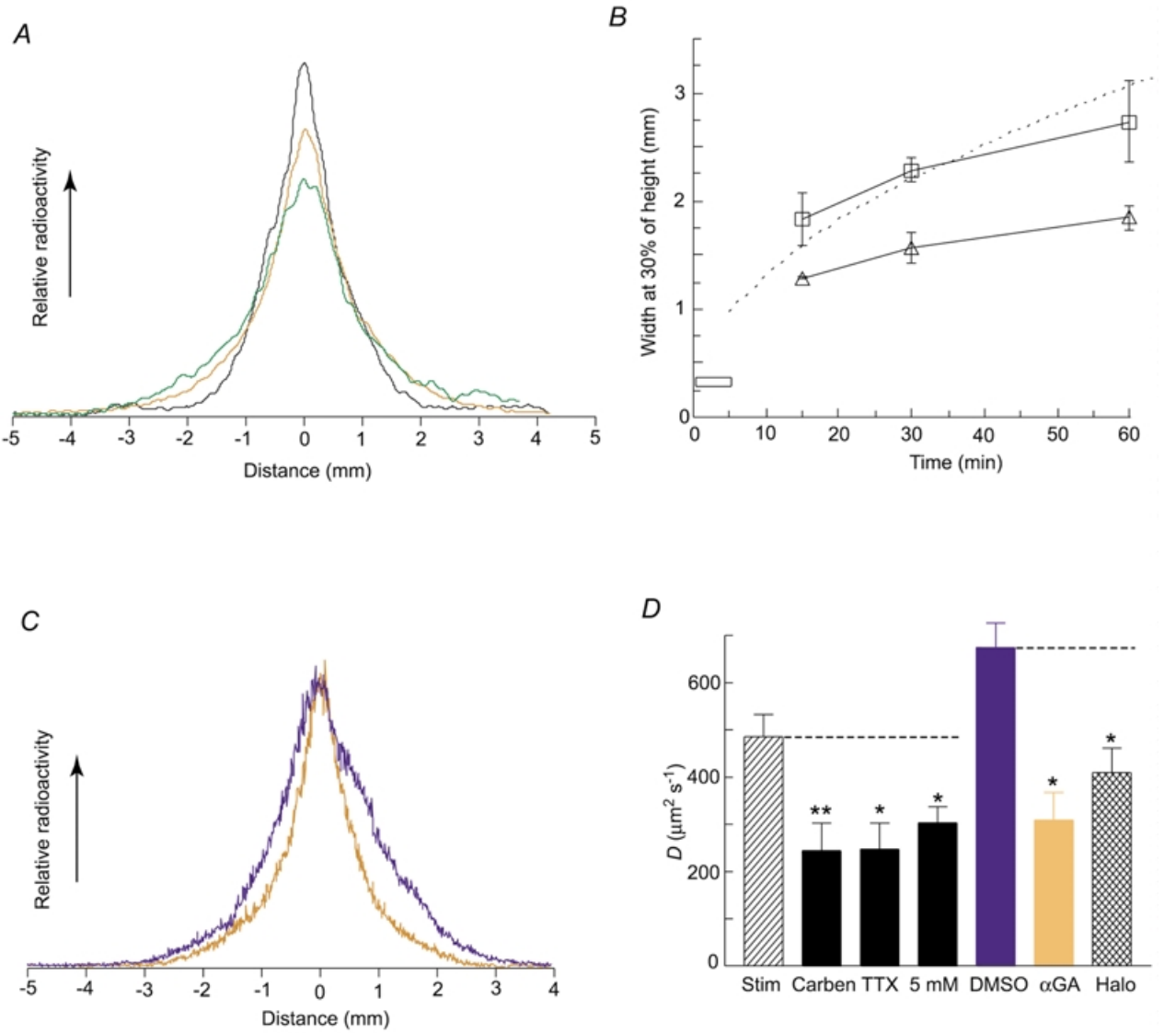

Figure 3. Characteristics of radioactivity profiles after local application of *DG

A, profiles after application of *DG for 5 min and incubation for 10 (black), 25 (orange) or 55 (green) min with stimulation. Individual profiles were normalized so that the area under each was the same, and then averaged for each time (2, 8 and 4 nerves respectively). *B*, the width of the peak at 30 % of the maximum height (*W*30) is plotted as a function of time from the beginning of the 5 min application of *DG. *W*30 for nerves in the presence of TTX (triangles) was less than for nerves that carried action potentials (squares). The height of the rectangle at time zero indicates the mean width of the Evans blue mark ± S.E.M., and its length the duration of the application. The dashed line is a theoretical calculation of *W*30 for diffusion of a substance with a diffusion coefficient of 470 $\mu m^2\ s^{-1}$; this value is an estimate, extrapolated from the literature, of the diffusion coefficient of DG-6P within a cell (see Discussion). *C*, experimental modification of the diffusion of radioactivity from *DG. In the presence of 18-α-glycerrhetinic acid (orange) the width of the profile was less than in control solution containing DMSO (blue). *DG was applied for 5 min and the nerves incubated for 25 min, with electrical stimulation. Two profiles were normalized and averaged for each condition. *D*. The profile for each nerve was characterized by fitting a diffusion curve for a single compartment with a coefficient *D* (see Fig. 4*A* and Appendix). The histogram shows mean values of *D* under different conditions, all for 5 min application of *DG and 25 min incubation. Bars indicate S.E.M. * $P < 0.05$, ** $P < 0.01$. 'Stim', stimulated in the absence of drugs; 'Carben', carbenoxolone; 'Halo', halothane.

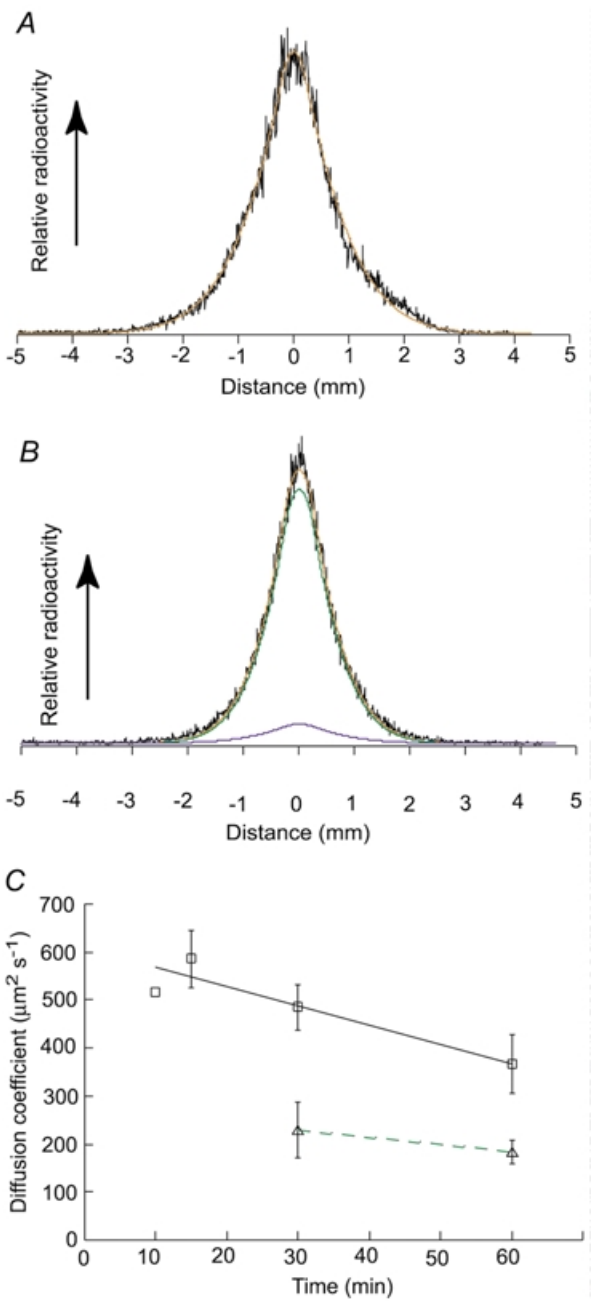

Figure 4. Fitting curves to calculate D

A, experimental profile (black) for a nerve under control conditions (30 min: application of *DG for 5 min followed by 25 min incubation during electrical stimulation). This profile was fitted with a calculated curve (orange) for a single compartment to obtain a value for *D*. In the presence of gap junction blockers, or, as in *B*, TTX, the profiles were narrowed (*B*, black line). The experimental profile was now better fitted as the sum (orange) of a small component that was not slowed (blue) and a slow component (green). *C*, mean values for different incubation times of diffusion coefficients used to fit profiles. The mean values of *D* for the single-compartment analysis of nerves stimulated in the absence of drugs are plotted as squares. Bars are S.E.M. values and there was only one value for 10 min. The line is a linear regression through the data points, $r^2 = 0.27$. Mean values for the diffusion coefficient, D_2, of the slower component used to fit profiles from TTX experiments are shown by triangles. (The components were not clearly resolved in the available profiles for 15 min).

all with the same diffusion coefficient, *D*. The curves were calculated for application of *DG for the actual finite time (5 min) over the length marked by the Evans blue in a nerve of finite length (Fig. 4*A*; see Appendix). *D* fell significantly ($P = 0.041$) over the incubation times used (5–55 min, squares in Fig. 4*C*). The mean value, for all the incubation times used (5–55 min) was $463 \pm 34\ \mu m^2\ s^{-1}$, $n = 16$ (or $0.46 \times 10^{-5}\ cm^2\ s^{-1}$).

That the curves could be well fitted by a single diffusion coefficient suggests three possibilities: (1) all the radioactive products (mainly *DG-6P) were in the axons; (2) all the radioactive products were in the Schwann cells; (3) radioactive products diffused with approximately the same (macroscopic) diffusion coefficient in both axons and Schwann cells.

As summarized in Fig. 3*D*, the profiles were narrower for nerves exposed to blockers of gap junctions (carbenoxolone and αGA) or to TTX, which abolished electrical activity. Although calculating a single mean diffusion coefficient for each profile enabled us to quantify these effects (Fig. 3*D*), two reasons led us to use a model with two compartments, one compartment with a greater diffusion coefficent D_1 and a second compartment with a smaller coefficient D_2, as described in the Appendix. The first reason was that, although the single compartment model was satisfactory under control conditions, the two-compartment model gave better fits in all cases where overall diffusion was slower than in the control conditions. The second reason was a matter of logic. Since there are no gap junctions along axons, and there is evidence that there are gap junctions between non-myelinating Schwann cells (see Discussion), it is likely that the diffusion that was reduced was occurring in a Schwann cell syncytium. It follows that some of the radioactive products of *DG were in the Schwann cells. We call this fraction λ; the rest of the radioactive products, which were presumably in the axons, correspond to the fraction $(1 - \lambda)$. To keep the number of parameters to be estimated small, we set D_1 to the mean value of *D* measured for the control conditions (Fig. 4*A* and *B*). This left two parameters, D_2 and λ to be estimated. As seen in Table 1, the profiles that were modified by carbenoxolone gave a mean value for λ of 73 %. Although the mean value of λ in the presence of TTX was slightly higher (85 %) the difference was not significant.

The results with αGA were treated slightly differently because the carrier, DMSO, by itself, increased the apparent *D* (the curves still being fitted with a single coefficient; Fig. 3*D*, Table 1). We therefore used this increased value of *D* as D_1 in the two-compartment model. The value of λ, 0.77 (Table 1) was not significantly different from that for carbenoxolone, so it seemed to make little difference whether the blocker was present during the *DG application (αGA) or only added afterwards, during the incubation (carbenoxolone).

Table 1. Diffusion and distribution of radioactive compounds in nerves

Conditions	D_1 ($\mu m^2 s^{-1}$)	D_2 ($\mu m^2 s^{-1}$)	λ	n
Control, 30 min	485 ± 47	n.a.	n.a.	8
Carbenoxolone, 100 μM	(485)	204 ± 24	0.734 ± 0.064	4
TTX, 30 min	(485)	228 ± 58	0.848 ± 0.027	3
5 mM DG*	(485)	261 ± 27	0.727 ± 0.068	4
DMSO	674 ± 51.5	n.a.	n.a.	2
αGA (in DMSO)	(674)	254 ± 28	0.771 ± 0.092	2

Under control conditions (application of *DG for 5 and 25 min incubation), each profile was well-fitted with a single diffusion coefficient, on average 485 $\mu m^2 s^{-1}$. For 'carbenoxolone', 'TTX' and '5 mM' two coefficients were used, the larger one being set to 485 $\mu m^2 s^{-1}$ (= 4.85×10^{-6} $cm^2 s^{-1}$). λ is the fraction in the compartment of slower diffusion. Each profile in DMSO was well fitted by a single coefficient. The mean of the values was 674 $\mu m^2 s^{-1}$, which was used for the faster compartment for fitting the αGA profiles. n.a. = not applicable. Values are means ± S.E.M. except for the DMSO and αGA experiments, which were for paired experiments, the errors indicating the ranges.

Effect of changing the concentration of *DG

We also applied *DG at 5 mM, instead of the 1 mM usually used. For the standard conditions of electrical stimulation and 25 min incubation after the application, the width, *W*30, was less than that for applications at 1 mM ($P = 0.0038$). The values were 2.29 ± 0.11 mm, $n = 6$, for 1 mM *DG and 1.67 ± 0.10 mm, $n = 4$, for 5 mM *DG. When the profiles were analysed in terms of two components, the D_2 and λ were similar to those obtained with 1 mM *DG in the presence of blockers.

Distribution of radioactivity after localized uptake of [^{14}C]glucose

The basis of the *DG method is the expectation that glucose is (or would be) taken up into the same cells (Sokoloff *et al.* 1977), although, of course, in the case of glucose, it is possible that metabolites (notably lactate) are transferred from one cell to another (Véga *et al.* 1998). As a test of our analysis of the radioactivity profiles after application of *DG, we compared the profiles after application of *DG with the profiles produced by application, in the same way, of *glucose at 2 mM for 5 min followed by incubation for 1–55 min. After incubation for 25 min, the quantity of radioactivity was, typically, about one-third that for the nerves exposed to *DG (after correction for the difference in specific activities). This is in qualitative agreement with the earlier observation that labelled compounds, notable CO_2 and lactate, leave the nerve (Véga *et al.* 1998).

The profiles were very variable, and, among 25 nerves, we observed no systematic effects of different conditions, such as presence of TTX, or different times of incubation (see below). Radioactivity was detectable within a few minutes all along the nerve, and on 19 of 25 nerves there was a narrow peak at the site of application (Fig. 5*A* and *B*, black profiles). On 10 nerves there were one or more very narrow peaks remote from the site of application (Fig. 5*A*, arrow; Fig. 5*C*, black profile). The width of the peak at the site of application, was measured at 30 % of the height of the peak above the plateau to give *W*30. Unlike the bell-shaped peak observed after application of *DG, there was no sign that the peak for *glucose broadened with time; linear regression of *W*30 on time showed no significant slope (mean: 0.0042 mm min^{-1}, $r^2 = 0.0059$, 19 points). The mean *W*30 for 25 min incubation was 0.316 ± 0.052 mm, $n = 5$ (excluding one wide peak with *W*30 = 1.66 mm). This is less than one-sixth of *W*30 for *DG under the same conditions (*W*30 after *DG = 2.29 ± 0.11 mm, $n = 6$; $P < 0.0001$). The mean ratio of the area of the peak to the area of the plateau after 25 min incubation was 0.22 ± 0.13, $n = 6$.

To investigate the natures of the two classes of peaks observed after application of *glucose (the peaks at the site of application, and the remote and very narrow ones), we incubated sample nerves with enzymes (after they had been lyophilized and their radioactivity profiles recorded). The glycogen degrading enzyme, amylase, almost completely removed the peak of radioactivity at the site of application (Fig. 5*A*; $n = 6$). Incubation for 1 h in Locke solution alone did not do this, although there was loss of radioactivity all along the nerve (Fig. 5*B*, $n = 6$). The effect of this amylase treatment on nerves to which *DG had been applied was different. Incubation of the lyophilized nerve in Locke solution for 1 h reduced the peak by, on average, 43.0 ± 2.7 % ($n = 8$; Fig. 5*D*, orange profile). Subsequent treatment of the same nerves with amylase caused a further reduction of the peak by only 12.6 ± 3.2 % (Fig. 5*D*, green profile).

The very narrow peaks observed remote from the site of application in 10 nerves had widths at their bases of 155–1000 μm (Fig. 5*A* and *C*). In sample nerves they were not abolished by treatment with amylase, but were abolished after incubation in trypsin (Fig. 5*C*, orange). Trypsin did not generally reduce the peak at the site of application. We did not investigate these observations further; we suggest that the trypsin-sensitive radioactivity may have been due to incorporation of newly synthesized

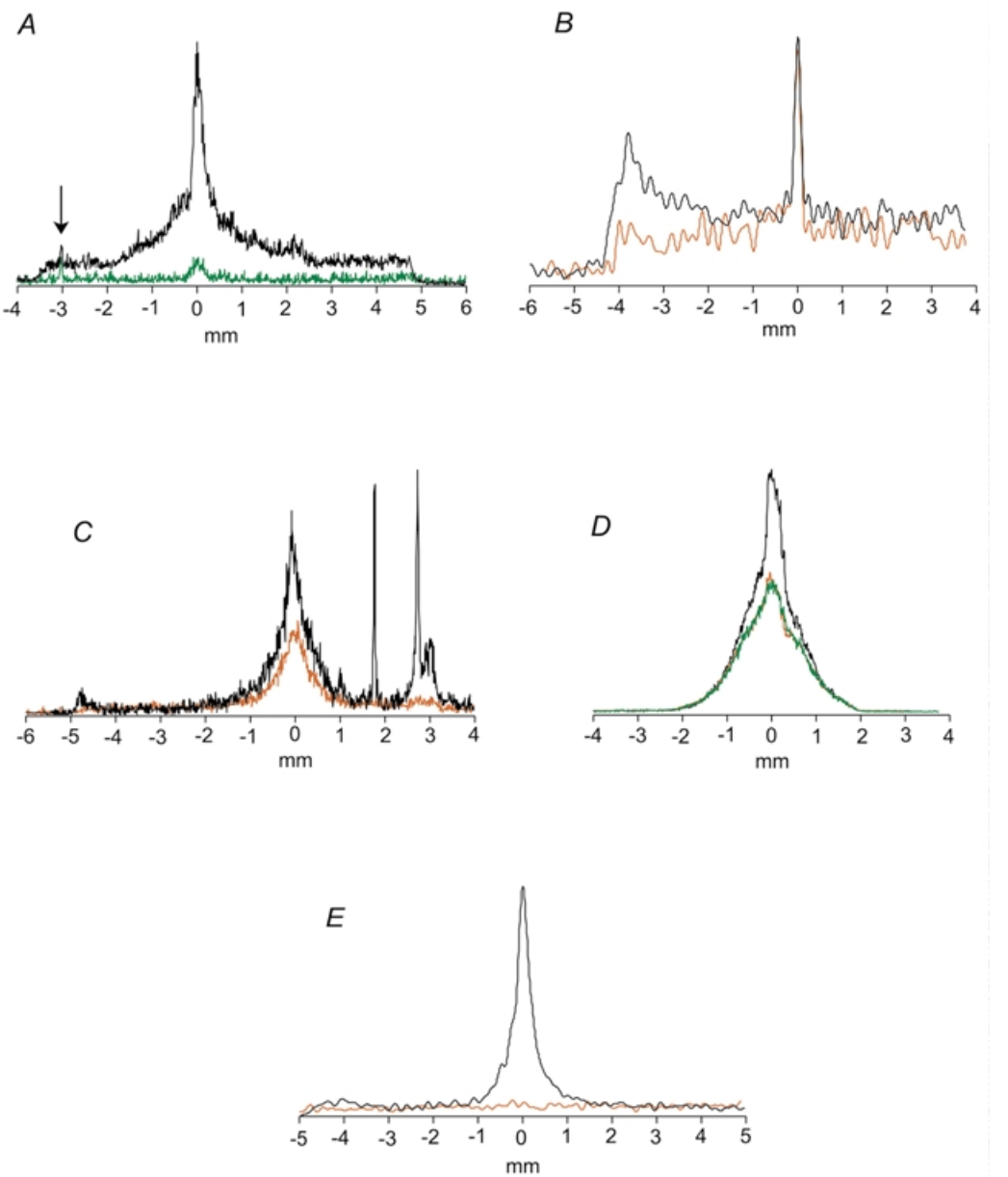

Figure 5. Typical profiles of radioactivity after uptake of [1-14C]d-glucose, and Na[U-14C]l-lactate

A, radioactivity profile of a nerve after incubation in [1-^{14}C]D-glucose (*glucose; black) showing weak radioactivity all along the nerve, with a peak at the site of application (at 0 mm). After treatment of the lyophilized nerve with amylase (green), the peak at the site of application was greatly reduced. A very small and narrow peak (arrow) was only slightly reduced by amylase. *Glucose was applied for 5 min followed by 25 min incubation with stimulation. *B*, profile from another nerve after application of *glucose (black). After incubation of the nerve in Locke solution (orange), the narrow peak at the site of application was not significantly reduced. Initially, *glucose had been applied for 5 min, and the nerve then incubated for 25 min, with stimulation. *C*, after application of *glucose, very narrow peaks remote from the site of application were sometimes observed (black). These were abolished by treatment with trypsin (orange). *Glucose was applied for 5 min followed by incubation for 25 min in the presence of TTX. *D*, profile after application of *DG (black). Incubation of the lyophilized nerve in Locke solution reduced the central peak (orange). A subsequent incubation in Locke solution containing amylase hardly changed the profile (green). *DG was applied for 5 min followed by 15 min incubation, without stimulation. *E*, profile after application of Na[U-^{14}C]L-lactate (*lactate; black). Treatment with amylase abolished the narrow peak at the site of application (orange). *Lactate was applied for 1 min followed by 14 min incubation with no stimulation.

amino acids into proteins at sites of damage, either near the cut ends of the nerve or where branches of the nerve were sectioned.

Absence of effect of cinnamate

If the axons have an absolute requirement for lactate, then blocking lactate transporters should impair the functioning of the axons and modify the metabolic fate of glucose supplied to the nerve. We tested the blocker α-cyano-4-hydroxy-cinnamate, which is a weak competitive inhibitor of monocarboxylic acid transporters on mitochondrial and plasma membranes (Halestrap & Price, 1999). α-Cyano-4-hydroxy-cinnamate (5 mM) was included in the perifusate solutions for experiments with the standard protocol: 5 min in zero glucose, 5 min application of *glucose, 25 min incubation in the presence of 5 mM glucose. We observed no evident differences in the maintenance of the action potential, or in the quantity of the radioactivity in the nerve or its distribution (five nerves, each paired with the contralateral nerve of the same rat). This absence of any marked effect of α-cyano-4-hydroxy-cinnamate in the presence of exogenous glucose is in agreement with the result of Wender *et al.* (2000) on optic nerve, and suggests that, in the presence of glucose, axons are able to function without lactate.

Distribution of radioactivity after localized uptake of [^{14}C]lactate

Application of [U-^{14}C]L-lactate (*lactate) gave results that we have not been able to distinguish clearly from those for *glucose. For shorter times (3–15 min) there was a peak at the site of application ($n = 12$). This peak did not broaden with time (0.0031 mm min^{-1}, $r^2 = 0.0076$) and its mean $W30$ was 0.851 ± 0.070 mm, $n = 13$, which is less than that of for *DG applied to nerves for 5 min followed by 10 min incubation in the presence of TTX ($P = 0.033$). In tests on four lyophilized nerves, this peak was abolished or greatly reduced by amylase (Fig. 5*E*). At 60 min no peak at the site of application was observed ($n = 5$); and there was an irregular plateau usually with a peak at one or both ends.

DISCUSSION

The Discussion focuses on the validity of our estimate that about 75 % of DG (and therefore glucose) was taken up by the Schwann cells under the conditions of these experiments. Our analysis compelled us to conclude that, in electrically stimulated nerves, the diffusion of DG-6P along the Schwann cell syncytium was, within the considerable imprecision of the method, as fast as diffusion along the axons. We were initially surprised by this result and consider it first.

Diffusion of radioactive products of *DG along the nerve

*DG and its metabolites diffused several millimetres along the nerve (Figs 2*B* and C, 3*A* and *B*). *DG, on entering a cell, is converted mainly to *DG-6P, and to a lesser extent to other charged compounds, which are trapped within the cell (Sokoloff *et al.* 1977; see below) which suggests that the diffusion was essentially intracellular. Further, if any *DG, or metabolite of *DG, were in the extracellular space at the end of the application it would have diffused rapidly to the bath. TTX applied at 1 μM in the bath abolished the action potentials in all the axons in about 1 min, indicating rapid access (see also Véga *et al.* 1998). If there were a uniform extracellular concentration of DG at the zone of application at the moment the application ended, then the concentration at the centre of the nerve would be expected to fall to below 1 % within 42 s. This figure was obtained using Fig. 5.3 in Crank (1975), a tortuosity factor of 1.6 (see Nicholson, 1995) and a diffusion coefficient of 600 μm^2 s^{-1}. Cellular uptake of DG, which would cause the fall in concentration to be even faster, has not been taken into account. Hence, on the time scale of our experiments, *DG and its radioactive metabolites must have been diffusing mainly within cells.

Compared to the control nerves, the diffusion profiles were narrowed when any of three different gap junction blockers was applied (Fig. 3*D*). There are no gap junctions along axons, but Schwann cells cultured from mouse vagus nerve express the gap junction proteins Connexin 32 and Connexin 43, and electrical coupling is observed between some pairs of cells (Zhao *et al.* 1999). In adult animals, electrical and dye coupling has been demonstrated between the astrocytes that ensheathe axons of amphibian optic nerve (Cohen, 1970; Marrero & Orkand, 1996). In the present experiments, we saw no signs of other possible effects of the gap junction blockers, such as a change in the amount of *DG taken up, or a decline of the action potential (although such effects would have had to be large to be detected). We conclude that at least part of the *DG-6P and the other labelled compounds were diffusing through Schwann cells. The observation that blocking electrical activity with TTX also narrowed the profiles (Fig. 3*B*) supports this conclusion. In frog optic nerve, electrical activity in the axons increases dye coupling between ensheathing glial cells (Marrero & Orkand, 1996), and Holthoff & Witte (2000) provide evidence that neuronal activity in rat neocortex increases coupling between astrocytes.

Was the rate of spread of the radioactivity along the nerves quantitatively compatible with intracellular diffusion? The major products of metabolism of DG in rat brain, identified by Dienel & Cruz (1993), are DG-6P (MW 244), and DG-1,6-P_2 (MW 338). In their experiments, after 45 min of infusion of *DG into the blood (with blood glucose concentration at 4.9 mM) DG-6P constituted 70 % of the total radioactivity, DG-1,6-P_2, 15 % and DG, 7 %; at shorter times, presumably, DG-6P and DG will be more predominant. Diffusion coefficients vary inversely with

approximately the 2/3 power of the molecular weight, so the coefficients for DG and DG-1,6P_2 will be roughly 1.3 and 0.8 times that of DG-6P. (Charge has little effect on apparent diffusion coefficients, at least in extracellular space (Nicholson & Phillips, 1981).) Hence, in a particular environment, we expect that *DG and its radioactive products will diffuse mainly with the diffusion coefficient of DG-6P, contaminated by small amounts of DG and DG-1,6-P_2, which move slightly faster and slower, respectively. Results obtained by radioactive labelling (Hodgkin & Keynes, 1953), recovery from photobleaching (Luby-Phelps *et al.* 1987), fluorescence correlation (Brock *et al.* 1998), and nuclear magnetic resonance (de Graaf *et al.* 2000) all show that molecules with diameters less than 20 nm have intracellular diffusion coefficients 80–90 % of those in free solution, so (calculating from the diffusion coefficient of glucose in free solution of 673 $\mu m^2 s^{-1}$) DG-6P is expected to have an intracellular diffusion coefficient of about 470 $\mu m^2 s^{-1}$. The mean value of D that fitted the profiles for stimulated nerves with 25 min incubation was not significantly different from this value (Table 1), and when $W30$ was calculated for diffusion using a coefficient of this value, the value agreed well at 30 min and was not significantly different at 15 and 60 min (Fig. 3*B*). This agreement implies that the labelled molecules were diffusing in an almost unobstructed intracellular space, i.e. that the gap junctions between one Schwann cell and the next offer relatively little resistance to macroscopic diffusion. We note that, along the diffusion path, a molecule passes from one cell to the next relatively infrequently, only once per 320 μm, and that the non-myelinating Schwann cells overlap, so that there are large areas of contiguous membrane. This overlapping, readily seen in electron micrographs of vagus nerve (not shown), has also been described in nerves of the rat bladder (Gabella, 1999).

There was a significant fall in the estimated value of D over the 5–55 min range of incubations times used (Fig. 4*C*). Over these times, an increasing fraction of DG-6P will have been converted to larger and less mobile molecules, including glycogen (Nelson *et al.* 1984; Dienel & Cruz, 1993), and perhaps some radioactive molecules became linked to enzymes. Such effects might account for the fall in D with time. But it seems unlikely that possible increases in such effects would account for the reduction in diffusion caused by gap junction blockers or by TTX. Our estimates of λ require simply that metabolism of DG in the axons be not very different from that in the Schwann cells.

Effects of DMSO and halothane

DMSO, used at 10^{-4} v/v as a carrier for αGA, increased the calculated value of D (Fig. 3*D*). A possible explanation is that DMSO acted on connective tissue to make it more elastic, so that the nerves were stretched on withdrawal from the bath and the increase in D is artifactual. Perhaps the halothane had a similar effect, which could explain why the net reduction in apparent D, although significant compared to nerves exposed to DMSO ($P = 0.03$), was not significant compared to control nerves ($P = 0.32$, see Fig. 3*D*).

Effect of increasing the concentration of *DG

When *DG was applied at 5 mM, instead of 1 mM, the profile was narrower (Fig. 3*D*), and this is reflected by the value of D_2 calculated by the model, which is similar to D_2 in the presence of gap junction blockers (Table 1). A conceivable contributing factor is that there would have been greater conversion of DG to DG-6P, a reaction that liberates protons. The cells would therefore acidify, and acidification is known to reduce coupling between ensheathing glial cells of amphibian optic nerve (Tang *et al.* 1985).

Profiles of radioactivity after applications of *glucose or *lactate

Of the six carbons of glucose, that in the 1 position is among those most likely to be trapped in amino acids or other metabolites, rather than being oxidized to CO_2 (Hawkins *et al.* 1985). It was therefore unsurprising that after application of [1-^{14}C]glucose, considerable radioactivity remained in the nerve. The profiles were irregular, but in many cases there was a peak at the site of application. These peaks were narrower than those observed after application of *DG, they did not broaden with time, and they were reduced, in lyophilized nerves, by treatment with amylase. These characteristics suggest that the peaks were composed of glycogen, which is more often encountered in glial cells than in neurons (Cataldo & Broadwell, 1986). In bee retina, incorporation of exogenous glucose into glycogen in glial cells is rapid and increased by neuronal activity (Evêquoz *et al.* 1983), and for mammalian brain, it has recently been suggested that glycogen is a major intermediate of glial cell metabolism (Shulman *et al.* 2001).

Metabolism of lactate to amino acids has been reported for rabbit vagus nerve (Véga *et al.* 1998) (and also for rat brain: Bouzier *et al.* 2000; Qu *et al.* 2000) so the presence of an irregular plateau of radioactivity after application of *lactate was not surprising. The profiles after application of *lactate usually included narrow amylase-sensitive peaks at the site of application. The rapidity of the oxidation of exogenous lactate in vagus nerve suggested to Véga *et al.* (1998) that lactate was taken up mainly by neurons, as is the case in rat brain (Bouzier *et al.* 2000), or when isolated or cultured astrocytes and neurons are compared (see Coles *et al.* 2000). However, the formation of glycogen from lactate by neural cells appears to have been described only for astrocytes in culture (Dringen *et al.* 1993*b*), which may suggest that some lactate in the present experiments was taken up by Schwann cells.

The proportion of locally applied glucose taken up by Schwann cells

Glucose has a greater affinity than DG for brain glucose transporters (Bachelard, 1971) and since the immediate product within the cell (glucose-6P) does not accumulate (unlike DG-6P) the Schwann cells should remove glucose from the extracellular clefts more effectively than they remove DG. Hence, if anything, for a given concentration outside the Schwann cells, even less glucose than DG is expected to reach the axons and be taken up by them (i.e. the fraction of glucose taken up by the Schwann cells was probably higher than the 78 % we estimate for the DG).

The proportion of glucose taken up by Schwann cells *in vivo*

The extracellular concentration of glucose in vagus nerve *in vivo* is unknown; in rat brain it has been measured as about 0.5 mM or less (Fellows *et al.* 1992; Lowry *et al.* 1998; Netchiporouk *et al.* 2001). In our experiments on desheathed nerve, the proportion of glucose extracted from the extracellular fluid by the Schwann cells as the glucose diffuses along the extracellular clefts towards the axons will be affected by the concentration of glucose outside the Schwann cell: the higher the concentration, the more glucose will escape capture and reach the axons. To discover the magnitude of this effect, we applied *DG at two concentrations, 1 and 5 mM. No significant difference was observed in the proportion taken up by the Schwann cells (Table 1). If extracellular glucose concentration in vagus nerve is as low as in the brain, then, if anything, a further correction in favour of uptake by Schwann cells should be made.

Two aspects of the way we applied *DG that we know were abnormal were that the application was over only a short length of a nerve, and that the nerve was deprived of glucose for 5 min before the application and during the 5 min of application, a total of 10 min. If the *DG taken up by Schwann cells at the site of application were able to diffuse away into Schwann cells unloaded by *DG then the uptake might be more avid than in normal conditions. This effect would tend to increase λ. However, in the experiments with αGA and with TTX, overall diffusion in the Schwann cells during application of *DG was reduced to about half (Table 1). This blocking would tend to oppose any artifactual increase in λ. Concerning the absence of exogenous glucose during the local application of *DG, we can only say that is striking that the Schwann cells still took up most of the *DG. It is the axons rather than the Schwann cells that appear to have the greater need for ATP: Ritchie (1967) concluded that 'all, or nearly all, of the energy derived from the resting oxygen consumption of nerve may well be devoted to the active transport of.....ions' (by the axons) (see also Attwell & Laughlin, 2001) and about 83 % of the mitochondria are in the axons (unpublished counts on electron micrographs). Perhaps, when the axons are less deprived of substrate, the Schwann cells take up an even higher proportion of the glucose than our λ.

Although there is good evidence for the transfer of metabolic substrate from glial cells to photoreceptors in bee retina (Tsacopoulos *et al.* 1988) and to the inner segments of vertebrate photoreceptors (Poitry-Yamate *et al.* 1995), to our knowledge, the present results (together with the preliminary results of Wittendorp-Rechenmann *et al.* (2002) for anaesthetized brain), are the first to offer a quantitative estimate of the high proportion of glucose that is taken up by glial cells. The results point strongly to a net, steady state, transfer of energy substrate from Schwann cells to neurons both in the absence of stimulation (in the presence of TTX) and when axonal energy requirements are increased by conduction of action potentials.

APPENDIX

Analysis of radioactivity profiles after application of *DG

*DG was applied to the nerve, approximately midway between its left and right extremities x_l and x_r, and uptake was uniform over a short length extending from $x_0 - a/2$ to $x_0 + a/2$. Under control conditions (stimulation at 2 Hz in the absence of drugs) a quantity Q was taken up, and *DG and its labelled products diffused intracellularly along the nerve with an apparent mean longitudinal diffusion coefficient D. In the presence of gap junction blockers, or TTX, a two-compartment model gave better fits: a quantity λQ entered a compartment with apparent diffusion coefficient D_2 and the remainder, $(1 - \lambda)Q$, entered a compartment with coefficient D_1, where $D_1 > D_2$. In the text, it is argued that the D_2 compartment corresponds mainly to diffusionally coupled (non-myelinating) Schwann cells, and the D_1 compartment corresponds to axons. We were unable to distinguish D_1 from D, i.e. under control conditions, $D_1 \approx D_2 \approx D$.

List of symbols for physical quantities

Q: total quantity of *DG taken up by the nerve, in arbitrary units; fraction λQ by the D_2 compartment (Schwann cells) and the remainder, $(1 - \lambda)Q$, by the D_1 compartment (axons).

$X(x,t)$: quantity of radioactivity (in arbitrary units) on diffusible molecules within the nerve, per unit length (for the one-compartment model) or in the D_1 compartment (for the two-compartment model).

$Y(x,t)$: quantity of radioactivity on diffusible molecules in the D_2 compartment per unit length of nerve.

x_l, x_r: left and right extremities of the nerve.

x_0: centre of segment length a of nerve to which radioactive substrate was applied.

D_1, D_2: mean apparent coefficients of longitudinal diffusion of diffusible radioactive molecules along axons and along Schwann cell space.

T_0: the duration of the application of *DG.

Diffusion in one compartment

The spread of radioactivity along the nerve is described by the differential equation:

$$\frac{\partial X(x,t)}{\partial t} = D\frac{\partial^2 X(x,t)}{\partial t^2} + \frac{Q}{a}(H(x - x_0 + a/2) - H(x_0 + a/2 - x))S(t), \qquad \text{(A1)}$$

where $H(x)$ is the Heaviside function:

$$H(x) = \begin{cases} 1 & \text{if} \quad x \geqslant 0 \\ 0 & \text{if} \quad x < 0. \end{cases}$$

$$S(t) = \frac{H(t) - H(t - T_0)}{T_0}.$$

Boundary conditions

At $t = 0$, the nerve contains no labelled compounds:

$$X(x,0) = 0.$$

There is zero flux across the ends of the nerve:

$$\frac{\partial X}{\partial x}(x_l,t) = 0 \qquad \frac{\partial X}{\partial x}(x_r,t) = 0. \qquad \text{(A2)}$$

Solution of eqn (A1)

We consider first the case of an instantaneous application of labelled substrate so that eqn (A1) becomes:

$$\frac{\partial X}{\partial t} = D\frac{\partial^2 X}{\partial x^2} + Q\frac{[H(x_0 + a/2) - H(x_0 - a/2)]}{a}\delta(t), \qquad \text{(A3)}$$

where $\delta(t)$ is the Dirac function. To satisfy the boundary conditions of eqn (A2), we introduce an infinite set of functions defined by:

$$\phi_k(x) = \cos\left(\frac{k\pi}{L}(x - x_l)\right) \qquad k = 0, 1, \ldots$$

where k is an integer and $L = x_r - x_l$ is the total length of the nerve. It can be shown that:

$$\frac{d\phi_k}{dx}(x_l) = 0 \qquad \frac{d\phi_k}{dx}(x_r) = 0 \qquad k = 0, 1, \ldots$$

The functions ϕ_k have the orthogonality property:

$$\int_{x_r}^{x_l} \phi_k(x)\phi_j(x)dx = \begin{cases} L/2 & \text{if} \quad k = j \neq 0 \\ 0 & \text{if} \quad k \neq j, k \neq 0, j \neq 0, \\ L & \text{if} \quad k = j = 0 \end{cases}$$

Boundary conditions (eqn (A2)) can be satisfied by any Fourier series expansion of functions ϕ_k. We write:

$$X(x,t) = \sum_{k=0}^{\infty} \alpha_k(t)\phi_k(x).$$

From eqn (A3), the α_k can be found from:

$$\frac{d\alpha_k(t)}{dt} = -\left(\frac{k^2\pi^2}{L^2}D\right)\alpha_k(t) + Qw_k\delta(t), \qquad \text{(A4)}$$

$$\alpha_k(0) = 0$$

with:

$$w_k = \begin{cases} \text{if} \quad a \neq 0 & \begin{cases} 1/L & \text{if} \quad k = 0 \\ (4/k\pi a)\sin(k\pi a/2L)\phi_k(x_0) & \text{if} \quad k \neq 0 \end{cases} \\ \text{if} \quad a = 0 & \begin{cases} 1/L & \text{if} \quad k = 0 \\ (2/L)(\phi_k(x_0)) & \text{if} \quad k \neq 0 \end{cases} \end{cases}$$

The solution of eqn (A4) is:

$$\alpha_k(t) = Qw_k \exp(-\mu_k t)H(t),$$

with:

$$\mu_k = \frac{k^2\pi^2}{L^2}D.$$

The solution of the original eqn (A1), which we denote $\bar{X}(x,t)$, is the convolution of $X(x,t)$ with the supply function $S(t)$:

$$\bar{X}(x,t) = \int_0^{\infty} X(x,t-\tau)S(\tau)d\tau = \frac{1}{T_0}\int_0^{\min(T_0,t)} X(x,t-\tau)d\tau$$

Since $X(x,t)$ is absolutely and uniformly convergent with respect to the variable x, for $t > 0$, we obtain:

$$\bar{X}(x,t) = \frac{Q}{T_0}\sum_{k=0}^{\infty}\frac{w_k}{\mu_k}\{\exp(\mu_k(\min(T_0,t) - t) - \exp(-\mu_k t)\}\phi_k(x)$$

Fitting the profiles

The apparent diffusion coefficient, D, was calculated in two steps: (1) T_0, t and a were experimentally known constants and the total amount of radioactivity, Q, was estimated as the integral of the radioactivity profile; (2) the central position, x_0, and D were obtained by minimizing the deviation between the model and the profile defined as:

$$E(D,x_0) = \frac{1}{i_r - i_l + 1}\sum_{i=i_l}^{i_r}(R_i - \bar{X}(x_i,t))^2,$$

where R_i is the specific radioactivity; i_l (i_r) is the index of the left (right) end of the nerve. The minimum of E was found using the Levenberg-Marquardt algorithm.

Two-compartment analysis

The same method was used to determine the second diffusion coefficient D_2 and the partition parameter λ in the two-compartment model. The full equations were:

$$\frac{\partial X(x,t)}{\partial t} =$$

$$D_1 \frac{\partial^2 X(x,t)}{\partial t^2} + \lambda \frac{Q}{a}[H(x - x_0 + a/2) - H(x_0 + a/2 - x)]S(t),$$

$$\frac{\partial Y(x,t)}{\partial t} = D_2 \frac{\partial^2 Y(x,t)}{\partial t^2} + (1-\lambda)\frac{Q}{a}[H(x - x_0 + a/2) - H(x_0 + a/2 - x)]S(t). \quad \text{(A5)}$$

Using a Fourier expansion for X and Y, we obtain the solution:

$$\bar{X}(x,t) =$$

$$(1-\lambda)\frac{Q}{T_0}\sum_{k=0}^{\infty}\frac{w_k}{\mu_k}\{\exp(\mu_k(\min(T_0,t)-t) - \exp(-\mu_k t)\}\phi_k(x),$$

$$\bar{Y}(x,t) = \lambda\frac{Q}{T_0}\sum_{k=0}^{\infty}\frac{w_k}{\nu_k}\{\exp(\nu_k(\min(T_0,t)-t) - \exp(-\nu_k t)\}\phi_k(x),$$

with:

$$\mu_k = \frac{k^2\pi^2}{L^2}D_1, \qquad \nu_k = \frac{k^2\pi^2}{L^2}D_2.$$

Fitting the profiles by the two-compartment model

The deviation between model and experiment was defined as:

$$E(D_2,\lambda) = \frac{1}{i_r - i_l + 1}\sum_{i=i_l}^{i_r}(R_i - \bar{X}(x_i,t) - \bar{Y}(x_i,t))^2,$$

where R_i is the radioactivity per unit length; i_l (i_r) is the index of the left (right) end of the nerve. The minimum of E which gave the best parameter fit was found using the Levenberg-Marquardt algorithm.

REFERENCES

Attwell D & Laughlin SB (2001). An energy budget for signaling in the grey matter of the brain. *J Cereb Blood Flow Metab* **21**, 1133–1145.

Bachelard HS (1971). Specificity and kinetic properties of monosaccharide uptake into guinea pig cerebral cortex *in vitro*. *J Neurochem* **18**, 213–222.

Bouzier AK, Thiaudiere E, Biran M, Rouland R, Canioni P & Merle M (2000). The metabolism of [3–^{13}C]lactate in the rat brain is specific of a pyruvate carboxylase-deprived compartment. *J Neurochem* **75**, 480–486.

Brock R, Hink MA & Jovin TM (1998). Fluorescence correlation microscopy of cells in the presence of autofluorescence. *Biophys J* **75**, 2547–2557.

Brooks GA (2002). Lactate shuttles in nature. *Biochem Soc Trans* **30**, 258–264.

Cataldo AM & Broadwell RD (1986). Cytochemical identification of cerebral glycogen and glucose-6-phosphatase activity under normal and experimental conditions: neurons and glia. *J Elect Microsc Tech* **3**, 413–437.

Chih CP, Lipton P & Roberts EL Jr (2001). Do active cerebral neurons really use lactate rather than glucose? *Trends Neurosci* **24**, 573–578.

Cohen MW (1970). The contribution by glial cells to surface recordings from the optic nerve of an amphibian. *J Physiol* **210**, 565–580.

Coles JA, Vega C & Marcaggi P (2000). Metabolic trafficking between cells in nervous tissue. *Prog Brain Res* **125**, 241–254.

Crank J (1975). *The Mathematics of Diffusion*. Oxford University Press, Oxford.

Davidson, JS & Baumgarten IM (1988). Glycyrrhetinic acid derivatives: a novel class of inhibitors of gap-junctional intercellular communication. Structure-activity relationships. *J Pharmacol Exp Ther* **246**, 1104–1107.

de Graaf RA, van Kranenburg A & Nicolay K (2000). *In vivo* ^{31}P-NMR diffusion spectroscopy of ATP and phosphocreatine in rat skeletal muscle. *Biophys J* **78**, 1657–1664.

Dienel GA & Cruz NF (1993). Synthesis of deoxyglucose-1-phosphate, deoxyglucose-1,6,-bisphosphate, and other metabolites of 2-deoxy-D-[^{14}C]glucose in rat brain *in vivo*: influence of time and tissue glucose level. *J Neurochem* **60**, 2217–2231.

Dringen R, Gebhardt R & Hamprecht B (1993*a*). Glycogen in astrocytes: possible function as lactate supply for neighboring cells. *Brain Res* **623**, 208–214.

Dringen R, Schmoll D, Cesar M & Hamprecht B (1993*b*). Incorporation of radioactivity from [^{14}C]lactate into the glycogen of cultured mouse astroglial cells. Evidence for gluconeogenesis in brain cells. *Biol Chem Hoppe Seyler* **374**, 343–347.

Evêquoz V, Stadelmann A & Tsacopoulos M (1983). The effect of light on glycogen turnover in the retina of the intact honeybee drone (*Apis mellifera*). *J Comp Physiol* **150**, 69–75.

Fellows LK, Boutelle MG & Fillenz M (1992). Extracellular brain glucose levels reflect local neuronal activity: a microdialysis study in awake, freely moving rats. *J Neurochem* **59**, 2141–2147.

Fox PT, Raichle ME, Mintun MA & Dence C (1988). Nonoxidative glucose consumption during focal physiologic neural activity. *Science* **241**, 462–464.

Gabella G (1999). Structure of the intramural nerves of the rat bladder. *J Neurocytol* **28**, 615–637.

Gjedde A, Marrett S & Vafaee M (2002). Oxidative and nonoxidative metabolism of excited neurons and astrocytes. *J Cereb Blood Flow Metab* **22**, 1–14.

Halestrap AP & Price NT (1999). The proton-linked monocarboxylate transporter (MCT) family: structure, function and regulation. *Biochem J* **343**, 281–299.

Hawkins RA, Mans AM, Davis DW, Vina JR & Hibbard LS (1985). Cerebral glucose use measured with [^{14}C]glucose labeled in the 1, 2, or 6 position. *Am J Physiol* **248**, C170–176.

Hodgkin AL & Keynes RD (1953). The mobility and diffusion coefficient of potassium in giant squid axons from *Sepia*. *J Physiol* **119**, 513–518.

Holthoff K & Witte OW (2000). Directed spatial potassium redistribution in rat neocortex. *Glia* **29**, 288–292.

Larrabee MG (1992). Extracellular intermediates of glucose metabolism: fluxes of endogenous lactate and alanine through extracellular pools in embryonic sympathetic ganglia. *J Neurochem* **59**, 1041–1052.

Larrabee MG & Horowicz P (1956). Glucose and oxygen utilization in sympathetic ganglia. I. Effects of anesthetics. II Substrates for oxidation at rest and in activity. In *Molecular Structure and Functional Activity of Nerve Cells*, pp. 84–107. American Institute of Biological Science, Washington.

Lowry JP, O'Neill RD, Boutelle MG & Fillenz M (1998). Continuous monitoring of extracellular glucose concentrations in the striatum of freely moving rats with an implanted glucose biosensor. *J Neurochem* **70**, 391–396.

Luby-Phelps K, Castle PE, Taylor DL & Lanni F (1987). Hindered diffusion of inert tracer particles in the cytoplasm of mouse 3T3 cells. *Proc Natl Acad Sci U S A* **84**, 4910–4913.

McIlwain H (1953). Glucose level, metabolism, and response to electrical impulses in cerebral tissues from man and laboratory animals. *Biochem J* **55**, 618–624.

Marrero H & Orkand RK (1996). Nerve impulses increase glial intercellular permeability. *Glia* **16**, 285–289.

Nelson T, Kaufman EE & Sokoloff L (1984). 2-Deoxyglucose incorporation into rat brain glycogen during measurement of local cerebral glucose utilization by the 2-deoxyglucose method. *J Neurochem* **43**, 949–956.

Netchiporouk L, Shram N, Salvert D & Cespuglio R (2001). Brain extracellular glucose assessed by voltammetry throughout the rat sleep-wake cycle. *Eur J Neurosci* **13**, 1429–1434.

Nicholson C (1995). Extracellular space as the pathway for neuron-glial cell interaction. In *Neuroglia*, ed. Kettenmann H & Ransom BR, pp. 387–397. Oxford University Press, Oxford.

Nicholson C & Phillips JM (1981). Ion diffusion modified by tortuosity and volume fraction in the extracellular microenvironment of the rat cerebellum. *J Physiol* **321**, 225–257.

Pellerin L & Magistretti PJ (1994). Glutamate uptake into astrocytes stimulates aerobic glycolysis: a mechanism coupling neuronal activity to glucose utilization. *Proc Natl Acad Sci U S A* **91**, 10625–10629.

Peyronnard JM, Terry LC & Aguayo A (1975). Schwann cell internuclear distances in developing rat unmyelinated nerve fibers. *Arch Neurol* **32**, 36–38.

Pfeuffer J, Tkác I, Choi I-Y, Merkle H, Ugurbil K, Garwood M & Gruetter R (1999). Localized *in vivo* ^{1}H NMR detection of neurotransmitter labeling in rat brain during infusion of [1–^{13}C] D-glucose. *Magn Reson Med* **41**, 1077–1083.

Poitry-Yamate CL, Poitry S & Tsacopoulos M (1995). Lactate released by Müller cells is metabolized by photoreceptors from mammalian retina. *J Neurosci* **15**, 5179–5191.

Qu H, Haberg A, Haraldseth O, Unsgard G & Sonnewald U (2000) ^{13}C MR spectroscopy study of lactate as substrate for rat brain. *Dev Neurosci* **22**, 429–436.

Ritchie JM (1967). The oxygen consumption of mammalian non-myelinated nerve fibres at rest and during activity. *J Physiol* **188**, 309–329.

Ritchie JM & Straub RW (1956). The after-effects of repetitive stimulation on mammalian non-medullated fibres. *J Physiol* **137**, 698–711.

Rozental R, Srinivas M & Spray DC (2001). How to close a gap junction channel. Efficacies and potencies of uncoupling agents. *Methods Mol Biol* 154, 447-476.

Schurr A, West CA & Rigor BM (1988). Lactate-supported synaptic function in the rat hippocampal slice preparation. *Science* **240**, 1326–1328.

Shulman RG, Hyder F & Rothman DL (2001). Cerebral energetics and the glycogen shunt: neurochemical basis of functional imaging. *Proc Natl Acad Sci U S A* **98**, 6417–6422.

Sokoloff L, Reivich M, Kennedy C, Des Rosiers MH, Patlak CS, Pettigrew KD, Sakurada O & Shinohara M (1977). The [^{14}C]deoxyglucose method for the measurement of local cerebral glucose utilization: theory, procedure, and normal values in the conscious and anesthetized albino rat. *J Neurochem* **28**, 897–916.

Soltanpour N & Santer RM (1996). Preservation of the cervical vagus nerve in aged rats: morphometric and enzyme histological evidence. *J Auton Nerv Syst* **60**, 93–101.

Tang CM, Orkand PM & Orkand RK (1985). Coupling and uncoupling of amphibian neuroglia. *Neurosci Lett* **54**, 237–242.

Tsacopoulos M, Evequoz-Mercier V, Perrottet P & Buchner E (1988). Honeybee retinal glial cells transform glucose and supply the neurons with metabolic substrate. *Proc Natl Acad Sci U S A* **85**, 8727–8731.

Tsacopoulos M & Magistretti PJ (1996). Metabolic coupling between glia and neurons. *J Neurosci* **16**, 877–885.

Véga C, Poitry-Yamate CL, Jirounek P, Tsacopoulos M & Coles JA (1998). Lactate is released and taken up by isolated rabbit vagus nerve during aerobic metabolism. *J Neurochem* **71**, 330–337.

Walz W & Mukerji S (1988). Lactate production and release in cultured astrocytes. *Neurosci Lett* **86**, 296–300.

Wender R, Brown AM, Fern R, Swanson RA, Farrell K & Ransom BR (2000). Astrocytic glycogen influences axon function and survival during glucose deprivation in central white matter. *J Neurosci* **20**, 6804–6810.

Wittendorp-Rechenmann E, Lam CD, Steibel F, Lasbennes F & Nehlig A (2002). High resolution tracer targeting combining microautoradiographic imaging by cellular ^{14}C-trajectography with immunohistochemistry: a novel protocol to demonstrate metabolism of [^{14}C]2-deoxyglucose by neurons and astrocytes. *J Trace Microprobe Tech* **20**, 505–515.

Zhao S, Fort A & Spray DC (1999). Characteristics of gap junction channels in Schwann cells from wild-type and connexin-null mice. *Ann NY Acad Sci* **883**, 533–537.

Acknowledgements

We thank Drs C. Amourette and D. Fagret for radioactivity facilities, A. Gué and A. Verna for electron microscopy, J. Arsaut for technical help, M. Décorps for discussion and C. Segebarth for comments on the manuscript. David Serre and Aurelie Bajolet contributed as students.

Author's present address

C. Véga: CNRS UMR 7102, Université Pierre et Marie Curie – case 14, 9 Quai St Bernard, 75252 Paris cedex 05, France.